Experimental and Theoretical Study of Viscoelastic Dampers with Different Matrix Rubbers

Zhao Dong Xu, A.M.ASCE[1]; Ya Xin Liao[2]; Teng Ge[3]; and Chao Xu[4]

Abstract: Viscoelastic (VE) dampers are one of the most popular structural control devices, and serious efforts have been undertaken to develop their availability in civil engineering. However, the performance of VE dampers is dependent on the energy dissipation properties of VE materials. In this study, several kinds of VE materials based on different matrix rubbers were developed, and tests on VE dampers based on nitrile butadiene rubber (NBR) matrix and silicone rubber (SR) matrix were carried out. The results indicate that NBR matrix VE dampers have a high energy dissipation capacity, whereas SR matrix VE dampers have stable performance under different working conditions. To clarify the mechanical properties of VE dampers based on NBR and SR matrices, the equivalent higher-order fractional derivative model, which takes into account the effects of temperature and frequency simultaneously, is proposed. The numerical results using this model are in accord with experimental results. **DOI: 10.1061/(ASCE)EM.1943-7889.0001101.**

Author keywords: Viscoelastic damper; Mathematical model; Nitrile butadiene rubber; Silicone rubber.

Introduction

In recent years, considerable attention has been paid to research and development of structural control devices, with particular emphasis on the alleviation of wind and seismic responses of buildings. According to the relationship between control systems, external energy, structural vibration responses, and dynamic load information, structural vibration control can be categorized as passive, intelligent, or hybrid (Soong and Spencer 2002). Among available devices, shock absorption using viscoelastic (VE) dampers is an effective passive control method that has been widely studied by domestic and foreign experts because of their fine damping, cheap cost, and simple construction. VE dampers have been used in different kinds of structures to alleviate wind and seismic responses (Tsai and Lee 1993; Samali and Kwok 1995; Matsagar and Jangid 2005; Saidi et al. 2011).

To reveal the performance of VE dampers precisely, analytical and experimental studies of their behaviors have been carried out (Tsai 1994; Gluck et al. 1996; Xu et al. 2004; Mazza and Vulcano 2011). Furthermore, the analytical theory and design of VE dampers used in civil engineering structures have been studied (Chang et al. 1998; Park et al. 2004; Rashid Nicolescu 2008) using shaking table tests (Chang et al. 1995; Xu 2000; Min et al. 2004; Kasai 2008). This research shows that VE dampers have high energy dissipation capacity under wind and earthquake conditions and that their mechanical properties are influenced by ambient temperature, excitation frequency, and excitation amplitude.

Because the performance of VE dampers is significantly affected by external excitations and environmental factors, it is critical to build a mathematical model to simulate their mechanical behaviors taking account of excitation frequency and amplitude. The Maxwell and Kelvin models were the first such models introduced. Payne (2003) showed that VE dampers exhibit a correlation between dynamic displacement and that the Kraus model can be used to describe this behavior. Xu (2007) proposed an equivalent standard solid model to reflect the effects of environmental temperature and excitation frequency at the same time. Lewandowski and Chorazyczewski (2010) used the fractional Kelvin and fractional Maxwell models to describe the dynamic behavior of systems with VE dampers.

It has been demonstrated that the dynamic properties of VE dampers are determined by VE materials. Efforts have been made to improve the damping properties of these materials (Kishi et al. 2004; Patri et al. 2007; Rezaei et al. 2009). However, because most are used mainly in high-frequency vibration control, there is an urgent need to develop a new type of high-energy-consumption viscoelastic material suitable for vibration control in civil engineering structures which has low-frequency vibration characteristics. In the current study, nitrile butadiene rubber (NBR) matrix and silicone rubber (SR) matrix viscoelastic materials were developed, and VE dampers were manufactured using them. The dampers were then experimentally studied considering excitation frequency and amplitude. Finally, the equivalent higher-order fractional derivative model, which considers temperature and frequency effects simultaneously, was proposed. The numerical results achieved using this model are in good agreement with experimental results.

Experimental Study of VE Dampers

The tested VE dampers, shown in Fig. 1, consist of two VE layers, each 10 mm thick, vulcanized alternatively with three

[1]Professor, Key Laboratory of C&PC Structures of the Ministry of Education, Southeast Univ., Nanjing 210096, China (corresponding author). E-mail: xuzhdgyq@seu.edu.cn

[2]Research Assistant, Changjiang Institute of Survey, Planning, Design and Research, Wuhan 430014, China. E-mail: lyxviras@163.com

[3]Master Student, Key Laboratory of C&PC Structures of the Ministry of Education, Southeast Univ., Nanjing 210096, China. E-mail: seuergeteng@163.com

[4]Doctor Student, Key Laboratory of C&PC Structures of the Ministry of Education, Southeast Univ., Nanjing 210096, China. E-mail: xchcivil@Gmail.com

Note. This manuscript was submitted on August 7, 2015; approved on February 4, 2016; published online on April 4, 2016. Discussion period open until September 4, 2016; separate discussions must be submitted for individual papers. This paper is part of the ***Journal of Engineering Mechanics***, © ASCE, ISSN 0733-9399.

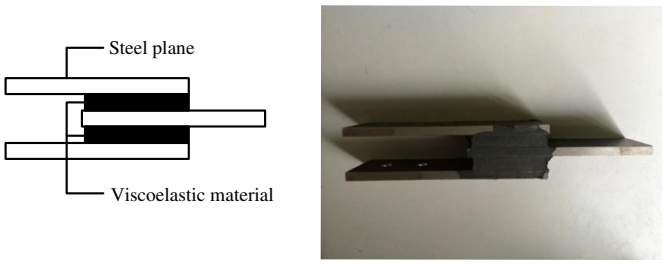

Fig. 1. Structure of a VE damper

Fig. 2. Test loading device

Table 1. Loading Conditions of VE Dampers

Frequency f (Hz)	Displacement amplitude d (mm)	Cycle number
0.1	1, 3, 5, 7, 10	10
0.2	1, 3, 5, 7, 10	10
0.5	1, 3, 5, 7, 10	10
1.0	1, 3, 5, 7, 10	10
1.5	1, 3, 5, 7, 10	10

steel plates, each 7 mm thick. The shear area of the VE layer is 3,000 mm^2.

Performance tests for the VE dampers with NBR matrix and SR matrix viscoelastic materials under different excitation frequencies and displacement amplitudes were conducted in a 10-ton servohydraulic testing machine in displacement control mode. The test loading device is shown in Fig. 2, and the loading conditions are listed in Table 1. The tests were carried out at 10.8°C ambient temperature.

Tests on the NBR Matrix Damper

Test results and hysteresis curves of the NBR matrix damper are shown in Figs. 3 and 4. It can be seen that the hysteresis curves are full ellipse, which means that this damper has fine energy dissipation capacity. It can also be seen that the curves' slope and plump degree are different under different excitation frequencies and amplitudes. This means that stiffness and damping change with excitation frequency and amplitude. Fig. 3 indicates that the enveloping area and the tilt angle of the hysteresis curves tend to increase when the excitation frequency increases, showing that energy dissipation capacity and stiffness increase with frequency. Fig. 4 indicates that the enveloping area of the hysteresis curves increases and their tilt angle decreases slightly when displacement amplitude increases.

Storage modulus G_1, loss modulus G_2, loss factor η, and energy dissipation E_d are the most important factors reflecting the properties of VE dampers. These factors can be obtained from the tested hysteresis curves. Under the sinusoidal excitation $u_d = u_0 \cdot \sin \omega t$, the relationship between damping force and excitation displacement can be expressed as

$$\left(\frac{F_d - K_{d1}u_d}{\eta K_{d1}u_0}\right)^2 + \left(\frac{u_d}{u_0}\right)^2 = 1 \tag{1}$$

$$G_1 = \frac{F_1 \cdot h_v}{nn \cdot A_v \cdot u_0} \tag{2}$$

$$\eta = \frac{F_2}{F_1} \tag{3}$$

$$G_2 = \eta \cdot G_1 \tag{4}$$

$$E_d = \pi u_0^2 G_2 \tag{5}$$

where F_d and u_d = damping force and excitation displacement, respectively; F_3 = largest damping force; u_0 = maximum displacement; F_1 = corresponding force at displacement u_0; F_2 = corresponding force at zero displacement ($F_2 = \eta K_{d1} u_0$), as shown in Fig. 5; K_{d1} = storage stiffness; G_1 = storage modulus; G_2 = loss modulus; η = loss factor; and E_d = energy dissipation.

In accordance with Eqs. (2)–(6), loss factor, storage modulus, loss modulus, and energy dissipation can be obtained from the tested hysteresis curves of the NBR matrix VE damper. These are listed in Table 2.

To reveal the effects of excitation frequency and displacement amplitude on the NBR matrix VE damper , storage modulus G_1, loss modulus G_2, loss factor η, and energy dissipation E_d under different frequencies are plotted in Fig. 6. It can be seen that G_1, G_2, η, and E_d increase with increasing frequency. Taking the amplitude of 10 mm as an example, the increasing ratios of storage modulus, loss modulus, loss factor, and energy dissipation are listed in Table 3. In summary, excitation frequency has an impact on the dynamic mechanical parameters of the NBR matrix VE damper.

Fig. 7 shows the relationship between dynamic characteristic factors and excitation displacement. It can be seen that with increasing displacement amplitude the characteristic factors G_1, G_2, and η decrease slightly whereas energy dissipation E_d increases. Taking the condition of 1.5 Hz as an example, the decreasing ratios of storage modulus, loss modulus, and loss factor are listed in Table 4. Energy dissipation increases with increasing displacement amplitude because it is proportional to the square of the deformation of the viscoelastic material. In summary, displacement amplitude has a slight impact on the dynamic mechanical parameters of the NBR matrix VE damper.

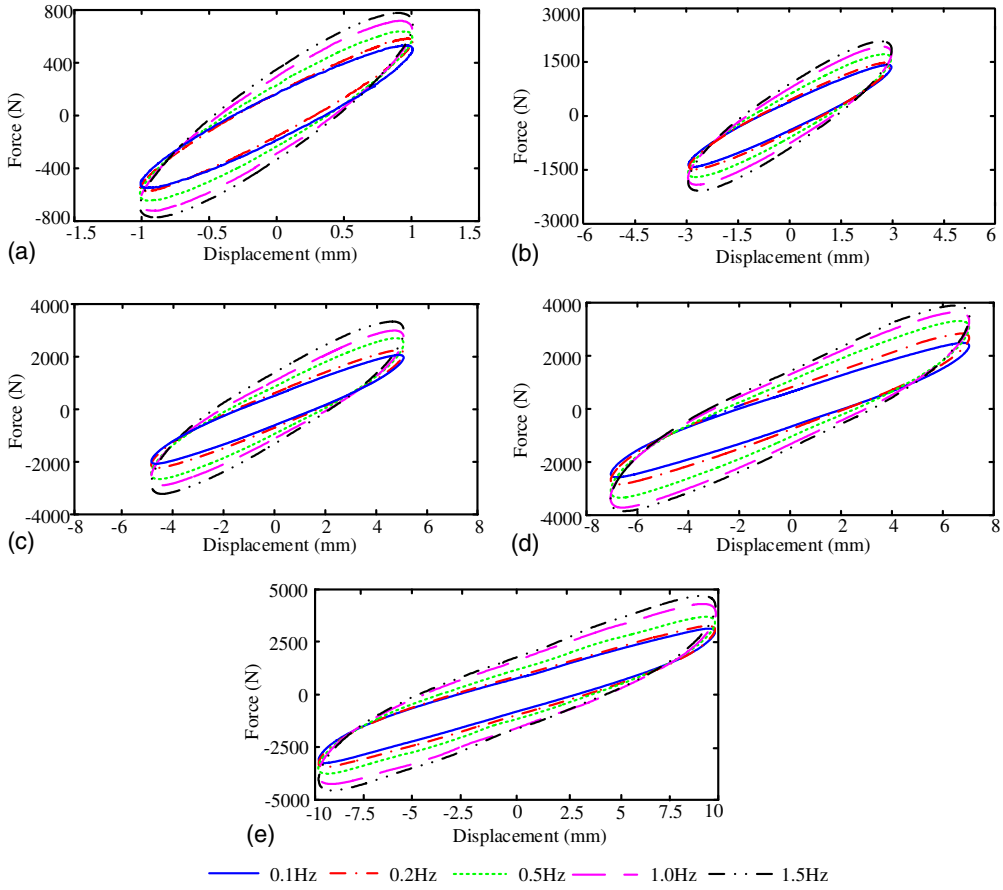

Fig. 3. Hysteresis curves of NBR damper change with excitation frequency: (a) $d = 1$ mm, $f = 0.1, 0.2, 0.5, 1.0, 1.5$ Hz; (b) $d = 3$ mm, $f = 0.1, 0.2, 0.5, 1.0, 1.5$ Hz; (c) $d = 5$ mm, $f = 0.1, 0.2, 0.5, 1.0, 1.5$ Hz; (d) $d = 7$ mm, $f = 0.1, 0.2, 0.5, 1.0, 1.5$ Hz; (e) $d = 10$ mm, $f = 0.1, 0.2, 0.5, 1.0, 1.5$ Hz

Tests on the SR Matrix Damper

Test results and hysteresis curves for the SR matrix damper are shown in Figs. 8 and 9. It can be seen that the hysteresis curves are not fuller than those of the NBR matrix VE damper. This means that the energy dissipation capacity of the SR matrix VE damper is worse than that of the NBR matrix VE damper. As seen in Fig. 8, the enveloping area and the tilt angle of the hysteresis curves change slightly when excitation frequency increases, The hysteresis curves are relatively stable when the excitation frequency changes. It can be seen from Fig. 9 that the enveloping area of the hysteresis curves increases and their tilt angle decreases when displacement amplitude increases. In accordance with Eqs. (2)–(6), loss factor, storage modulus, loss modulus, and energy dissipation can be obtained from the tested hysteresis curves of the SR matrix VE damper. These are listed in Table 5.

To show the effect of excitation frequency and displacement amplitude on the SR matrix VE damper, its storage modulus G_1, loss modulus G_2, loss factor η, and energy dissipation E_d under different frequencies are plotted in Fig. 10. It can be seen that G_1, G_2, η, and E_d are relatively stable with increasing frequency. Taking the amplitude of 10 mm as an example, increasing loss factor and energy dissipation ratios are listed in Table 6. Storage modulus and loss modulus are basically unchanged. In summary, excitation frequency has a slight impact on the dynamic mechanical parameters of the SR matrix VE damper.

Fig. 11 shows the relationship of the dynamic characteristic factors and excitation displacement. It can be seen that with increasing amplitude the characteristic factors G_1, G_2, and η decrease whereas energy dissipation E_d increases. Taking the excitation frequency of 1.5 Hz as an example, decreasing storage modulus, loss modulus, and loss factor ratios are listed in Table 7. As with the NBR matrix damper, and for the same reason, energy dissipation increases with increasing displacement amplitude. In summary, displacement amplitude has a slight impact on the dynamic mechanical parameters of the SR matrix VE damper and the damper's performance is relatively stable under different conditions.

As described before, NBR matrix VE dampers have more excellent energy dissipation capacity, and their maximum loss factor is up to 0.571. Buildings and machines usually gather a relatively large amount of energy when they are subjected to vibration, which means that these dampers are suitable for shock absorption in civil and/or mechanical engineering structures. Although the loss factor of SR matrix dampers is smaller compared with that of NBR matrix dampers, the performance and energy dissipation capacity of SR matrix dampers are relatively stable. Therefore, the developed SR matrix damper can adapt to the complex space environment and is suitable for shock absorption in aerospace structures.

Equivalent Higher-Order Fractional Derivative Model

The experimental results here and previous research show that the properties of VE dampers are affected by ambient temperature, excitation frequency, and displacement amplitude. Also, it can be seen from the analysis that displacement amplitude has a slight

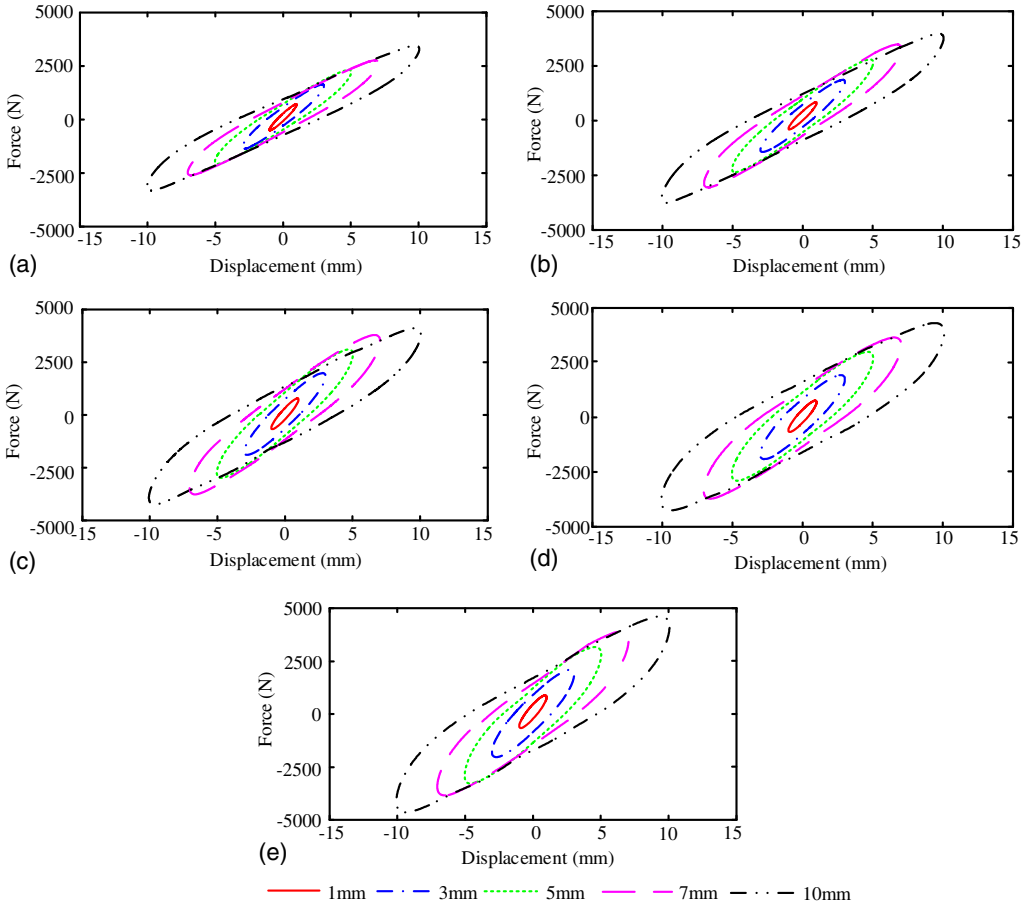

Fig. 4. Hysteresis curves of NBR damper change with displacement: (a) $f = 0.1$ Hz, $d = 1, 3, 5, 7, 10$ mm; (b) $f = 0.2$ Hz, $d = 1, 3, 5, 7, 10$ mm; (c) $f = 0.5$ Hz, $d = 1, 3, 5, 7, 10$ mm; (d) $f = 1$ Hz, $d = 1, 3, 5, 7, 10$ mm; (e) $f = 1.5$ Hz, $d = 1, 3, 5, 7, 10$ mm

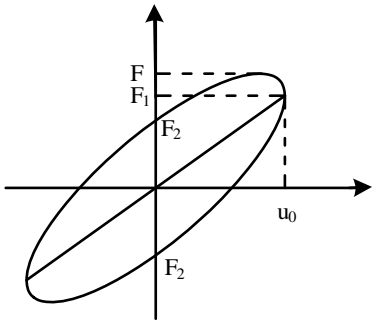

Fig. 5. Force-displacement hysteresis curve

effect on the dampers' dynamic parameters. Therefore, this effect is not considered in the following model. When the fractional derivative model is used, it should be improved to fit well with the experimental data, which increases its complexity and the number of parameters. The shortage is that the fractional derivative model need more parameters to fit well with the experimental data, which increases the complexity of model. Moreover, it contains three different fractional parameters and the maximum order of equations is more than one. Fractional derivatives make this model more accurate in simulating the creep and stress relaxation of viscoelastic materials, and thus the model can more accurately describe the materials' constitutive relations. To reflect the temperature on VE

Table 2. Characteristic Parameters of the NBR Matrix VE Damper

Frequency (Hz)	Amplitude (mm)	Loss factor (η)	Storage modulus G_1 (MPa)	Loss modulus G_2 (MPa)	Energy dissipation (N · m)
0.1	1	0.280	0.87	0.24	0.76
	3	0.311	0.72	0.22	6.33
	5	0.284	0.65	0.19	14.55
	7	0.267	0.55	0.15	22.68
	10	0.257	0.49	0.13	39.67
0.2	1	0.347	0.87	0.30	0.95
	3	0.319	0.74	0.24	6.66
	5	0.310	0.70	0.218	17.11
	7	0.297	0.63	0.19	28.79
	10	0.311	0.51	0.16	50.24
0.5	1	0.423	0.99	0.42	1.31
	3	0.381	0.88	0.34	9.50
	5	0.366	0.83	0.30	23.84
	7	0.345	0.73	0.25	38.50
	10	0.339	0.58	0.20	62.28
1	1	0.526	1.13	0.59	1.86
	3	0.459	0.95	0.44	12.34
	5	0.400	0.89	0.36	27.92
	7	0.391	0.77	0.30	46.63
	10	0.431	0.62	0.27	83.73
1.5	1	0.571	1.30	0.74	2.33
	3	0.511	1.01	0.51	14.52
	5	0.465	0.92	0.43	33.49
	7	0.450	0.86	0.39	59.38
	10	0.444	0.67	0.30	93.99

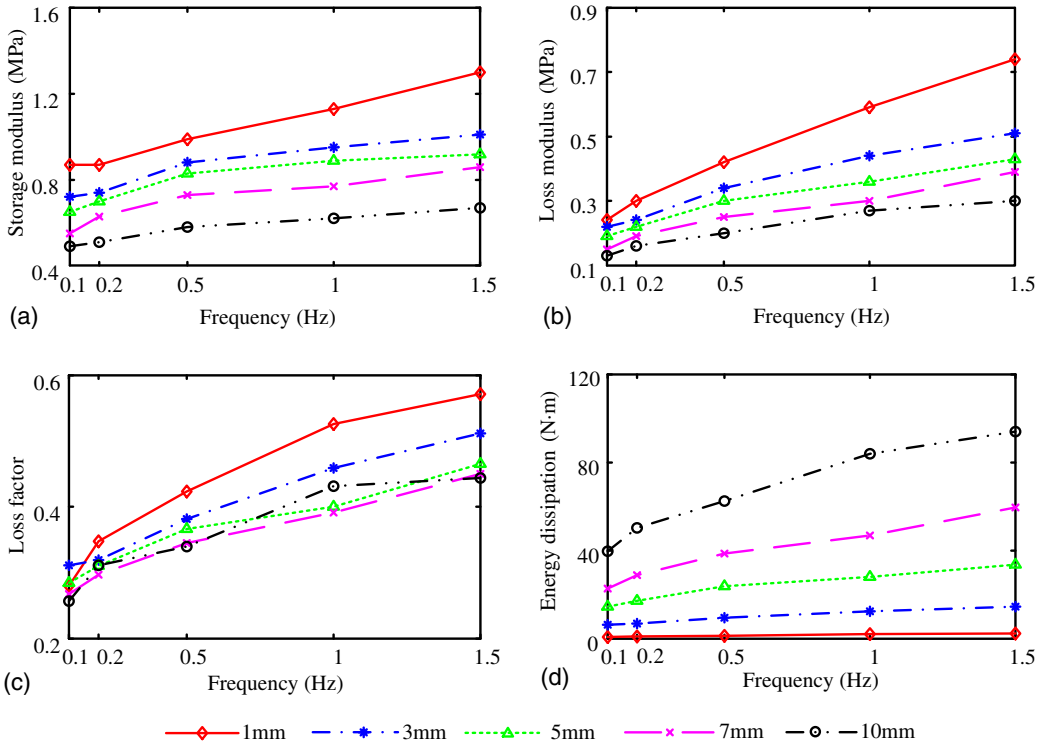

Fig. 6. Dynamic parameters of NBR damper changes with excitation frequency: (a) storage modulus; (b) loss modulus; (c) loss factor; (d) energy dissipation

Table 3. Change Rate of Characteristic Parameters of the NBR Matrix VE Damper

Amplitude (mm)	Frequency (Hz)	Storage modulus G_1	Loss modulus G_2	Loss factor η	Energy dissipation
10	0.1–0.2	+4.7%	+26.6%	+20.9%	+26.6%
	0.2–0.5	+13.5%	+23.9%	+9.2%	+23.9%
	0.5–1	+5.8%	+34.5%	+27.1%	+34.5%
	1–1.5	+9.1%	+12.3%	+2.8%	+12.3%

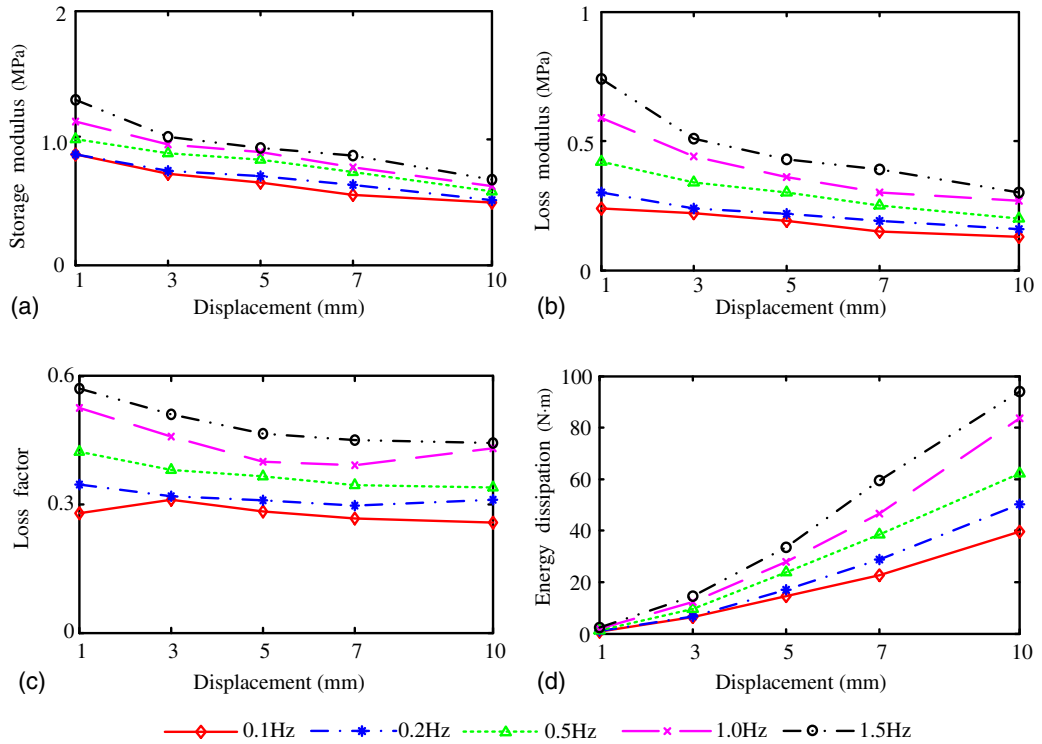

Fig. 7. Dynamic parameters of SR damper changes with displacement amplitude: (a) storage modulus; (b) loss modulus; (c) loss factor; (d) energy dissipation

Table 4. Change Rate of Characteristic Parameters of the NBR Matrix VE Damper

Frequency (Hz)	Amplitude (mm)	Storage modulus G_1	Loss modulus G_2	Loss factor η
1.5	1–3	−22.6%	−30.7%	−10.5%
	3–5	−8.6%	−16.9%	−9.1%
	5–7	−6.6%	−9.5%	−3.2%
	7–10	−21.4%	−22.4%	−1.4%

dampers, temperature-frequency equivalent theory is introduced into the higher-order fractional derivative model, which then becomes the equivalent higher-order fractional derivative model proposed in this study.

Theoretical Derivation

The higher-order fractional derivative model simulates VE dampers using fractional calculus, which consists of a fractional Maxwell model and a fractional Kelvin model in parallel, as shown in Fig. 12. The variables and μ_2 are the elastic modulus of the spring elements, and the variables η_1 and η_2 are the viscosity coefficients of the dash pots. The model can be written as Eq. (6), in which α, β, and γ are orders of fractional derivatives:

$$\frac{c_2}{c_1}\sigma(t)+\frac{1}{\eta_1}D^{\alpha}\sigma(t)=D^{\alpha+\gamma}\varepsilon(t)+c_1D^{\alpha}\varepsilon(t)+\frac{\mu_2}{\mu_1}D^{\beta}\varepsilon(t)+c_2D^{\gamma}\varepsilon(t)+c_1c_2\varepsilon(t)$$
$$c_1=\frac{\mu_1}{\eta_1},\qquad c_2=\frac{\mu_2}{\eta_2} \tag{6}$$

This equation can be expressed in standard mathematical form as

$$\sum_{m=0}^{M}b_mD^{\alpha_m}\sigma(t)=\sum_{n=0}^{N}E_nD^{\beta_n}\varepsilon(t) \tag{7}$$

where b_m and E_n = material parameters; and α_m and β_n = orders of fraction. When α_m and β_n are integers, the fractional derivative model can be transformed into a standard mathematical model. Thus, the higher-order fractional derivative model can cover the standard mathematical model well, the fractional derivative relations are closer to the viscoelastic rheological properties, and the model can precisely simulate VE damper mechanical behavior.

The following equation can be obtained by applying Fourier transformation on Eq. (6):

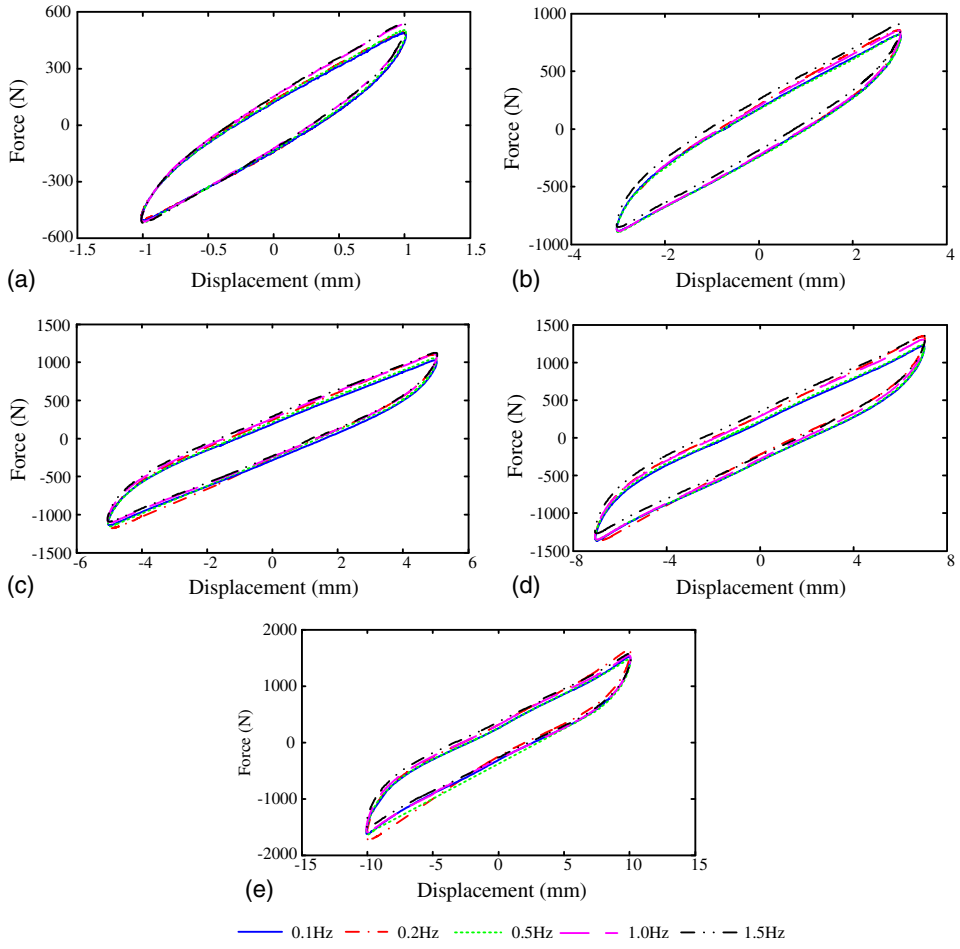

Fig. 8. Hysteresis curves of SR damper change with excitation frequency: (a) $d = 1$ mm, $f = 0.1, 0.2, 0.5, 1.0, 1.5$ Hz; (b) $d = 3$ mm, $f = 0.1, 0.2, 0.5, 1.0, 1.5$ Hz; (c) $d = 5$ mm, $f = 0.1, 0.2, 0.5, 1.0, 1.5$ Hz; (d) $d = 7$ mm, $f = 0.1, 0.2, 0.5, 1.0, 1.5$ Hz; (e) $d = 10$ mm, $f = 0.1, 0.2, 0.5, 1.0, 1.5$ Hz

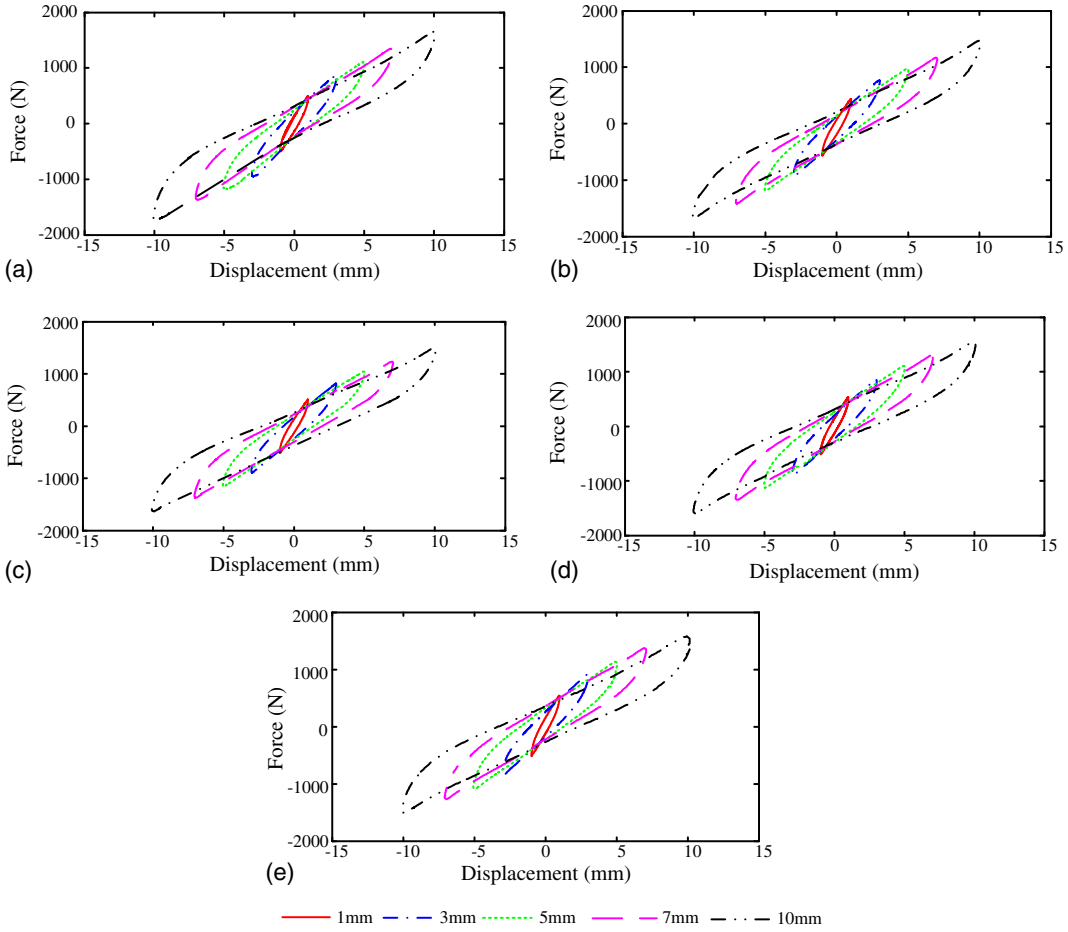

Fig. 9. Hysteresis curves of SR damper change with displacement: (a) $f = 0.1$ Hz, $d = 1, 3, 5, 7, 10$ mm; (b) $f = 0.2$ Hz, $d = 1, 3, 5, 7, 10$ mm; (c) $f = 0.5$ Hz, $d = 1, 3, 5, 7, 10$ mm; (d) $f = 1$ Hz, $d = 1, 3, 5, 7, 10$ mm; (e) $f = 1.5$ Hz, $d = 1, 3, 5, 7, 10$ mm

$$\frac{1}{\eta_1}[c_2 + (i\omega)^{\alpha}]\sigma(\omega) = \left[(i\omega)^{\alpha+\gamma} + c_1(i\omega)^{\alpha} + \frac{\mu_2}{\eta_1}(i\omega)^{\beta} + c_2(i\omega)^{\gamma} + c_1c_2\right]\varepsilon(\omega) \quad (8)$$

The complex modulus of viscoelastic materials can be obtained from Eq. (8):

$$G^*(\omega) = \frac{\sigma(\omega)}{\varepsilon(\omega)} = \mu_1 + \eta_1(i\omega)^{\gamma} + \mu_2\frac{(i\omega)^{\beta}}{c_2 + (i\omega)^{\alpha}} \quad (9)$$

The real and imaginary parts can be separated into the following equation:

$$G^*(\omega) = \mu_1 + \eta_1\omega^{\gamma}\cos\frac{\gamma\pi}{2} + \frac{\mu_2c_2\cos\frac{\beta\pi}{2} + \mu_2\omega^{\alpha}\cos\frac{(\alpha+\beta)\pi}{2}}{c_2^2 + 2c_2\omega^{\alpha}\cos\frac{\alpha\pi}{2} + \omega^{2\alpha}} + \left(\eta_1\omega^{\gamma}\sin\frac{\gamma\pi}{2} + \frac{\mu_2c_2\sin\frac{\beta\pi}{2} + \mu_2\omega^{\alpha}\sin\frac{(\alpha+\beta)\pi}{2}}{c_2^2 + 2c_2\omega^{\alpha}\cos\frac{\alpha\pi}{2} + \omega^{2\alpha}}\right)i \quad (10)$$

According to the relative theory of viscoelastic material (Xu 2000), the real part and the imaginary part are the storage modulus $G_1(\omega)$ and the loss modulus $G_2(\omega)$ of, respectively.

$$G_1(\omega) = \mu_1 + \eta_1\omega^{\gamma}\cos\frac{\gamma\pi}{2} + \frac{\mu_2c_2\cos\frac{\beta\pi}{2} + \mu_2\omega^{\alpha}\cos\frac{(\alpha+\beta)\pi}{2}}{c_2^2 + 2c_2\omega^{\alpha}\cos\frac{\alpha\pi}{2} + \omega^{2\alpha}} \quad (11)$$

Table 5. Characteristic Parameters of the SR Matrix VE Damper

Frequency (Hz)	Amplitude (mm)	Loss factor η	Storage modulus G_1 (MPa)	Loss modulus G_2 (MPa)	Energy dissipation (N · m)
0.1	1	0.307	0.79	0.24	0.76
	3	0.248	0.48	0.12	3.33
	5	0.218	0.37	0.08	6.28
	7	0.200	0.31	0.06	9.49
	10	0.183	0.25	0.05	14.60
0.2	1	0.254	0.81	0.21	0.64
	3	0.240	0.47	0.11	3.17
	5	0.224	0.35	0.078	6.12
	7	0.203	0.30	0.06	9.30
	10	0.190	0.25	0.048	14.97
0.5	1	0.261	0.84	0.22	0.69
	3	0.253	0.46	0.12	3.31
	5	0.229	0.35	0.08	6.36
	7	0.211	0.31	0.06	9.96
	10	0.197	0.25	0.05	15.28
1	1	0.259	0.84	0.22	0.68
	3	0.252	0.47	0.12	3.33
	5	0.231	0.36	0.08	6.59
	7	0.220	0.30	0.07	10.11
	10	0.204	0.25	0.05	16.17
1.5	1	0.267	0.88	0.23	0.73
	3	0.250	0.47	0.12	3.31
	5	0.240	0.36	0.09	6.72
	7	0.220	0.30	0.07	10.18
	10	0.221	0.25	0.05	17.01

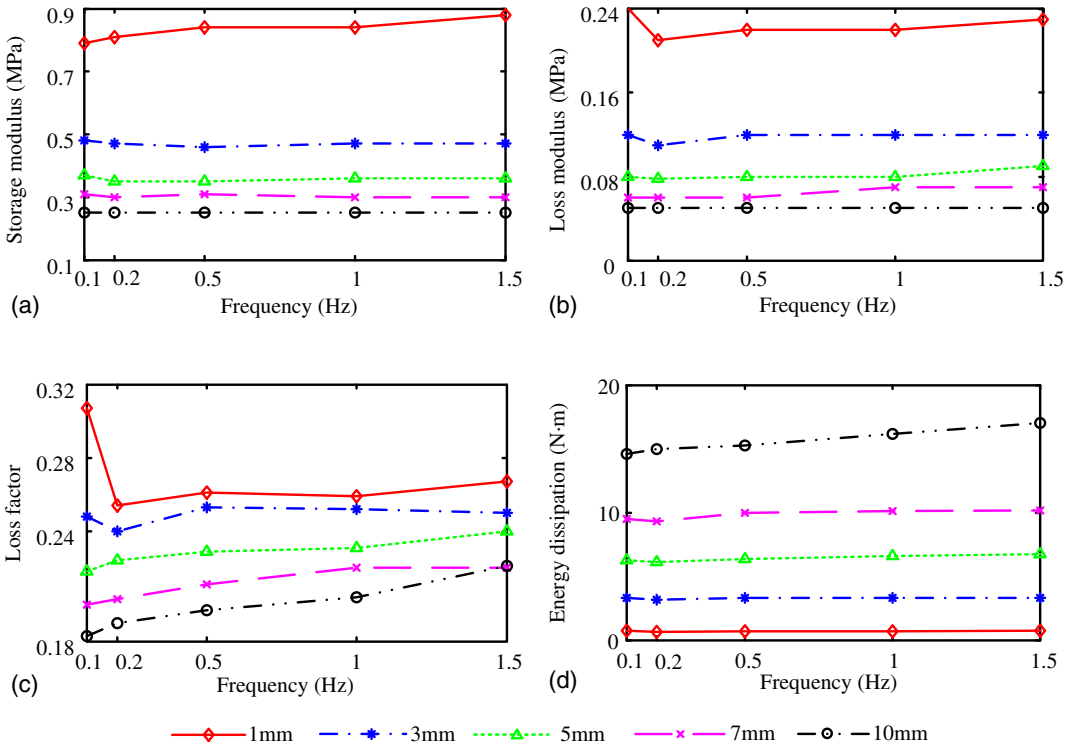

Fig. 10. Dynamic parameters of SR damper changes with excitation frequency: (a) storage modulus; (b) loss modulus; (c) loss factor; (d) energy dissipation

Table 6. Change Rate of Characteristic Parameters of the SR Matrix VE Damper

Amplitude (mm)	Frequency (Hz)	Loss factor η (%)	Energy dissipation (%)
10	0.1–0.2	+3.8	+2.5
	0.2–0.5	+3.7	+2.1
	0.5–1	+3.6	+5.8
	1–1.5	+8.3	+5.2

$$G_2(\omega) = \eta_1 \omega^{\gamma} \sin\frac{\gamma\pi}{2} + \frac{\mu_2 c_2 \sin\frac{\beta\pi}{2} + \mu_2 \omega^{\alpha} \sin\frac{(\alpha+\beta)\pi}{2}}{c_2^2 + 2c_2\omega^{\alpha}\cos\frac{\alpha\pi}{2} + \omega^{2\alpha}} \tag{12}$$

Xu (2007) found that the performance of VE dampers exhibits an equivalent relationship between high temperature and low frequency, which can be described by the temperature-frequency equivalent theory, as shown in Eq. (13). When this theory is introduced into the previous equations, storage modulus G_1, loss modulus G_2, and loss factor η can be obtained:

$$G_1(\omega, T) = G_1(\alpha_T\omega, T) \qquad \eta(\omega, T) = \eta(\alpha_T\omega, T)$$
$$\alpha_T = 10^{-12(T-T_0)/[525+(T-T_0)]} \tag{13}$$

$$\begin{aligned} G_1(\omega, T) = {} & \mu_1 c_2^2 + 2\mu_1 c_2 \alpha_T^{\alpha}\omega^{\alpha}\cos\frac{\alpha\pi}{2} + \mu_1\alpha_T^{2\alpha}\omega^{2\alpha} \\ & + \eta_1 c_2^2 \alpha_T^{\gamma}\omega^{\gamma}\cos\frac{\gamma\pi}{2} + 2\eta_1 c_2 \alpha_T^{\alpha+\gamma}\omega^{\alpha+\gamma}\cos\frac{\alpha\pi}{2}\cos\frac{\gamma\pi}{2} \\ & + \eta_1\alpha_T^{2\alpha+\gamma}\omega^{2\alpha+\gamma}\cos\frac{\gamma\pi}{2} + \mu_2 c_2\cos\frac{\beta\pi}{2} \\ & + \mu_2\alpha_T^{\alpha}\omega^{\alpha}\cos\frac{(\alpha+\beta)\pi}{2} \end{aligned} \tag{14}$$

$$\begin{aligned} G_2(\omega, T) = {} & \eta_1 c_2^2 \alpha_T^{\gamma}\omega^{\gamma}\sin\frac{\gamma\pi}{2} + 2\eta_1 c_2 \alpha_T^{\alpha+\gamma}\omega^{\alpha+\gamma}\sin\frac{\alpha\pi}{2}\sin\frac{\gamma\pi}{2} \\ & + \eta_1\alpha_T^{2\alpha+\gamma}\omega^{2\alpha+\gamma}\sin\frac{\gamma\pi}{2} + \mu_2 c_2\sin\frac{\beta\pi}{2} \\ & + \mu_2\alpha_T^{\alpha}\omega^{\alpha}\sin\frac{(\alpha+\beta)\pi}{2} \end{aligned} \tag{15}$$

$$\eta(\omega, T) = G_2(\omega, T)/G_1(\omega, T) \tag{16}$$

Equations (14)–(16) constitute formulas of the high-order equivalent fractional derivative model. The variables μ_1 and μ_2 are the elastic modulus of the spring elements; the variables η_1 and η_2 are the viscosity coefficients of the dash pots; and α, β, and γ are orders of fractional derivatives. These parameters can be obtained from experimental data. The variable α_T is the temperature shift factor, which converts the temperature effect into the frequency effect.

Experimental Verification

To verify the accuracy of the high-order equivalent fractional derivative model, storage modulus G_1 and loss factor η under different frequencies and temperatures are calculated in accordance with Eqs. (14)–(16). For the tested NBR matrix VE damper, some of the experimental data are used to determine the model parameters as $\mu_1 = 8.2 \times 10^3$, $\mu_2 = 3.5 \times 10^3$, $\eta_1 = 1.8$, $\eta_2 = 3.8 \times 10^4$, $\alpha = 0.58$, $\beta = 0.56$, $\gamma = 0.13$, and $T_0 = 70$°C in *MATLAB*. For the tested SR matrix VE damper, the parameters of the model are $\mu_1 = 2.8 \times 10^4$, $\mu_2 = 2.4 \times 10^2$, $\eta_1 = 0.28$, $\eta_2 = 1.8 \times 10^3$, $\alpha = 0.85$, $\beta = 0.61$, $\gamma = 0.35$, and $T_0 = 65$°C. The experimental data at an amplitude 10 mm of the VE dampers (the data that do not participate in parameter determination) are used to verify the model's numerical data.

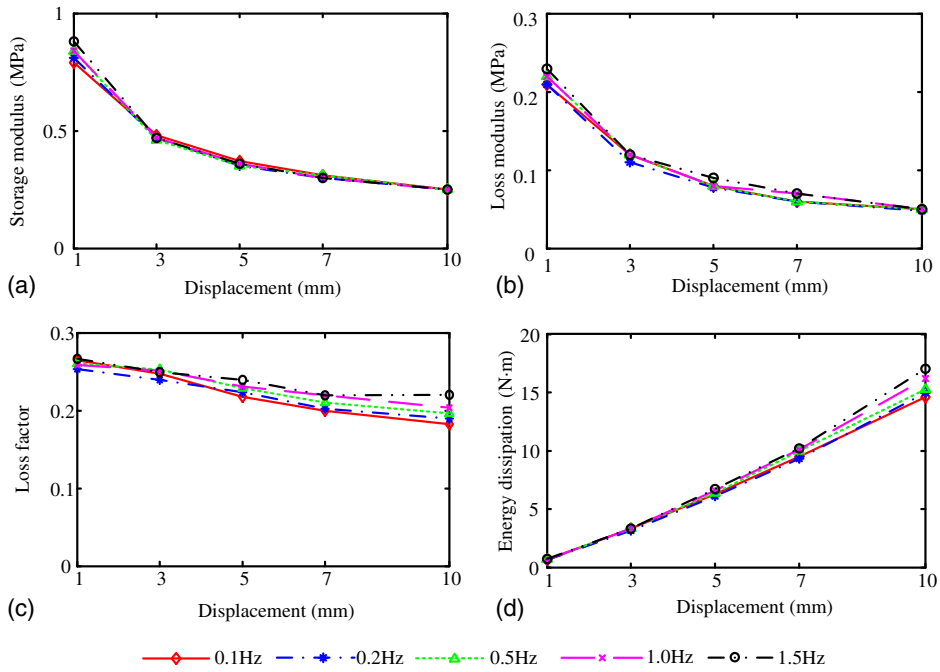

Fig. 11. Dynamic parameters of SR damper changes with displacement: (a) storage modulus; (b) loss modulus; (c) loss factor; (d) energy dissipation

Table 7. Change Rate of Characteristic Parameters of the SR Matrix VE Damper

Frequency (Hz)	Amplitude (mm)	Storage modulus G_1	Loss modulus G_2	Loss factor η
1.5	1–3	−26.5%	−29.8%	−6.1%
	3–5	−23.7%	−26.9%	−4.2%
	5–7	−15.8%	−22.7%	−2.3%
	7–10	−13.4%	−18.2%	−0.5%

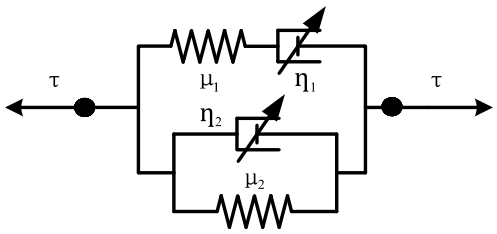

Fig. 12. Higher-order fractional derivative model

The experimental and numerical results of the equivalent standard solid model (ESSM) and the high-order equivalent fractional derivative model (EFDM) are summarized in Table 8 and plotted in Fig. 13. It can be seen that the high-order EFDM is better than the ESSM in describing the characteristics of VE dampers with different matrices. For example, the experimental value for NBR storage modulus is 0.492 MPa and for NBR loss factor is 0.257 when the excitation frequency is 0.1 Hz. The ESSM value for NBR storage modulus is 0.419 Mpa and for NBR loss factor is 0.269, whereas the EFDM value for NBR storage modulus is 0.490 Mpa and for NBR loss factor is 0.257. As can be seen, the numerical results of the EFDM agree better with the experimental values than do those of the ESSM, having an error of 0.4% for storage modulus and an error of 0.2% for loss factor. For the ESSM, the error for storage modulus is 14% and for loss factor is 4.7%.

To verify the temperature effect of the high-order EFDM, the experimental data (Xu 2000) for 9050 A and ZN22 VE materials under different frequencies and ambient temperatures are compared with the numerical data calculated by the ESSM

Table 8. Comparison of Experimental and Numerical Results for the NBR and SR Matrices

			Experimental value		Equivalent standard solid model		High-order equivalent fractional derivative model	
Materials	T (°C)	ω (Hz)	G_1(MPa)	η	G_1(MPa)	η	G_1(MPa)	η
NBR	13.2	0.1	0.492	0.257	0.419	0.269	0.490	0.257
	13.2	0.2	0.515	0.311	0.521	0.293	0.525	0.300
	13.2	0.5	0.585	0.339	0.647	0.337	0.580	0.363
	13.2	1	0.618	0.431	0.688	0.396	0.628	0.413
	13.2	1.5	0.675	0.444	0.649	0.465	0.658	0.443
SR	10.5	0.1	0.251	0.183	0.259	0.194	0.253	0.182
	10.5	0.2	0.257	0.190	0.253	0.193	0.247	0.189
	10.5	0.5	0.253	0.197	0.253	0.198	0.253	0.200
	10.5	1	0.252	0.204	0.256	0.203	0.258	0.209
	10.5	1.5	0.252	0.221	0.244	0.207	0.252	0.214

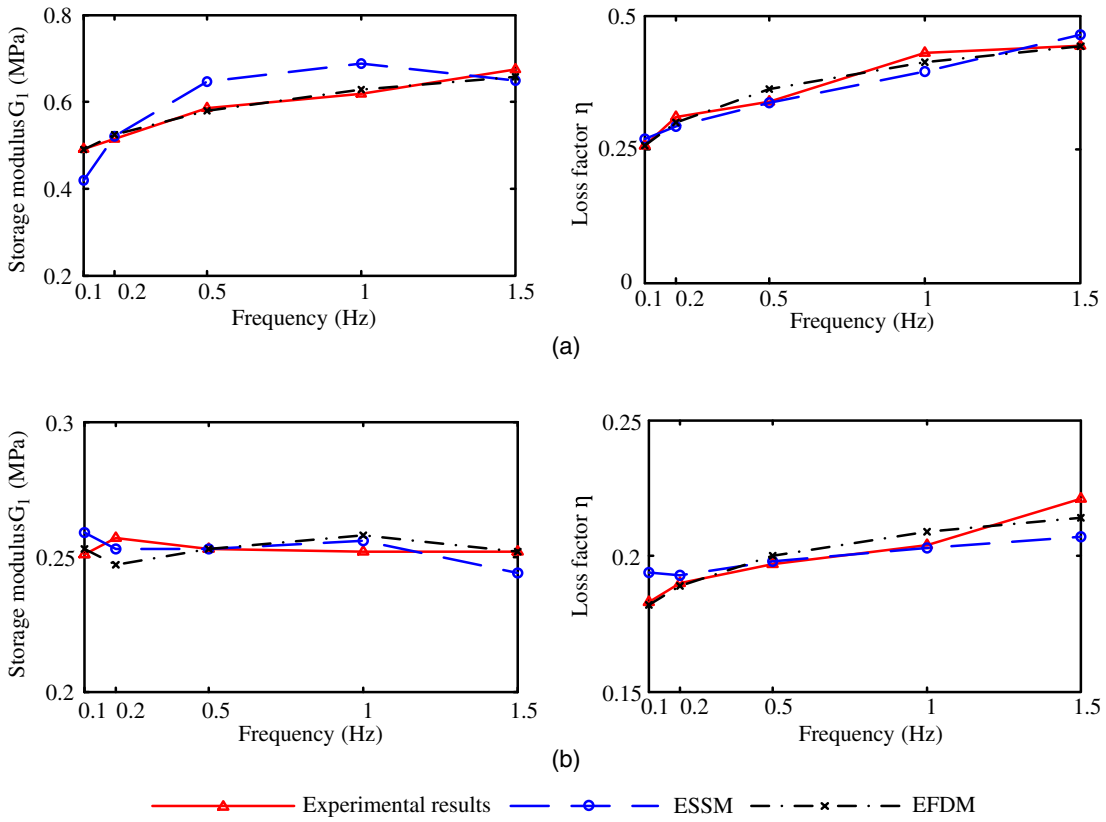

Fig. 13. Experimental and numerical results for materials based on NBR and SR: (a) experimental and numerical results compared at NBR matrix temperature 13.2°C; (b) experimental and numerical results compared at SR matrix temperature 10.5°C

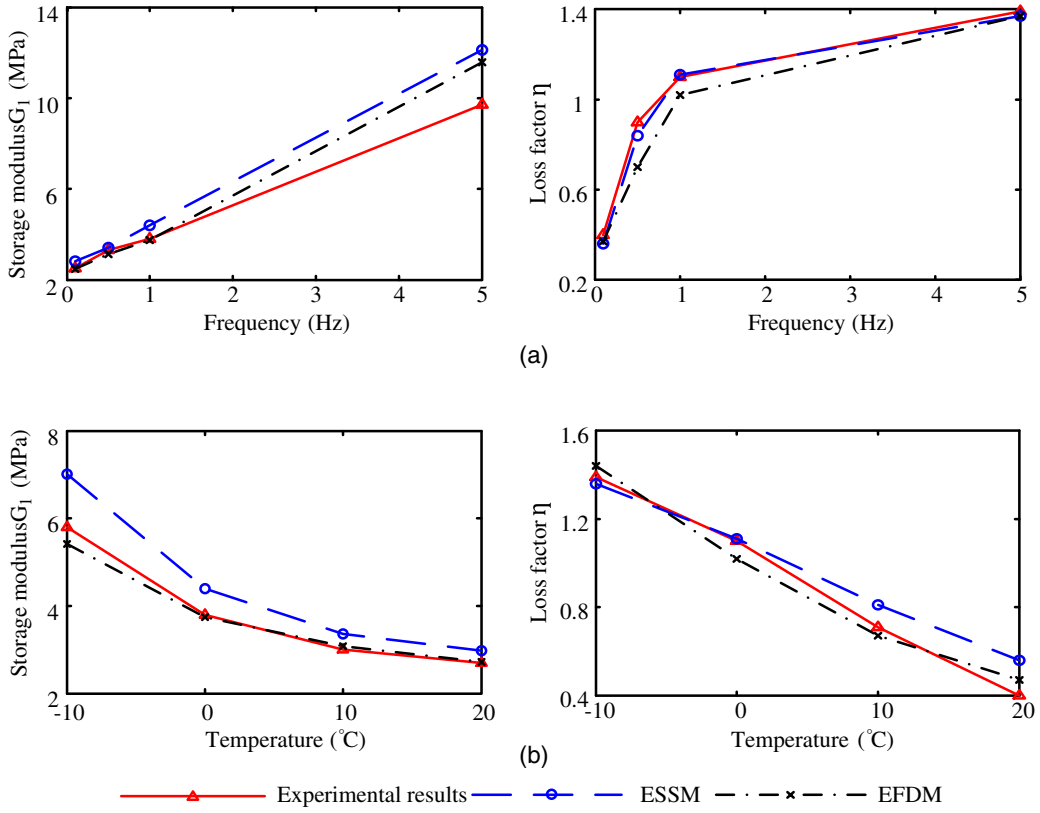

Fig. 14. Experimental and numerical results comparison of 9050A VE material: (a) experimental and numerical results compared at temperature 0°C; (b) experimental and numerical results compared at frequency 1.0 Hz

and the high-order EFDM. The ESSM (Xu 2011) is proposed to describe the effects of temperature and frequency on VE materials based on temperature-frequency equivalent theory and the standard linear solid model. Storage modulus G_1 and loss factor η are written as follows:

$$G' = (q_0 + p_1 q_1 \alpha_T^c \omega^c)/(1 + p_1^2 \alpha_T^c \omega^c)$$
$$\eta = (q_1 - p_1 q_0)\alpha_T^d \omega^d/(q_0 + p_1 q_1 \alpha_T^{2d} \omega^{2d})$$
$$\alpha_T = 10^{-12(T-T_0)/[525+(T-T_0)]} \quad (17)$$

where T_0 = reference temperature; c, d = parameters determined by the experimental data; and α_T = temperature conversion coefficient.

9050A VE material is based on a chlorinated butyl rubber matrix. Its accessory ingredients include mainly stearic acid, zinc oxide, accelerant dibenzothiazole disulfide (DM), calcium carbonate, general-purpose furnace black, and sulfur. ZN22 VE material is based on a bromide butyl rubber matrix. Its accessory ingredients include stearic acid, zinc oxide, accelerant tetramethylthiuram disulfide (TMTD), paraffin wax, high-abrasion furnace black, and sulfur. For 9050A VE material, the parameters of the high-order EFDM are determined to be $\mu_1 = 6.8 \times 10^3$, $\mu_2 = 1.5 \times 10^5$, $\eta_1 = 0.11$, $\eta_2 = 1.1 \times 10^4$, $\alpha = 0.52$, $\beta = 0.98$, $\gamma = 0.96$, and $T_0 = 91$°C. For ZN22 material, the parameters are $\mu_1 = 1.02 \times 10^3$, $\mu_2 = 6.17 \times 10^4$, $\eta_1 = 9.65$, $\eta_2 = 1.74 \times 10^3$, $\alpha = 0.63$, $\beta = 0.98$, $\gamma = 0.52$, and $T_0 = 102$°C.

Fig. 14 compares experimental and numerical results for 9050A VE material. It can be seen from Fig. 14(a) that the high-order EFDM is more accurate than the ESSM when describing storage modulus G_1 and loss factor η under different frequencies. For example, when the excitation frequency is 1.0 Hz, the experimental results show the storage modulus as 2.5 MPa and the loss factor as 0.4; the ESSM results show the storage modulus as 2.82 MPa and the loss factor as 0.36; and the EFDM results show the storage modulus as 2.47 Mpa and the loss factor as 0.37. For the ESSM,

Table 9. Maximum Value of Errors between Different Models

Dynamic characteristic factors of different materials	Equivalent standard solid model		High-order equivalent fractional derivative model	
	Maximum value	Average value	Maximum value	Average value
Storage modulus of 9050 A material	27.5	16.5	29.4	7.5
Loss factor of 9050 A material	40.0	9.6	22.2	7.6
Storage modulus of ZN22 material	41.9	19.7	22.7	11.4
Loss factor of ZN22 material	27.2	15.3	29.8	10.8
Storage modulus of NBR matrix	11.3	8.3	1.9	1.4
Loss factor of NBR matrix	4.9	4.8	7.1	2.9
Storage modulus of SR matrix	3.2	1.9	3.8	1.4
Loss factor of SR matrix	6.2	2.8	2.4	1.6

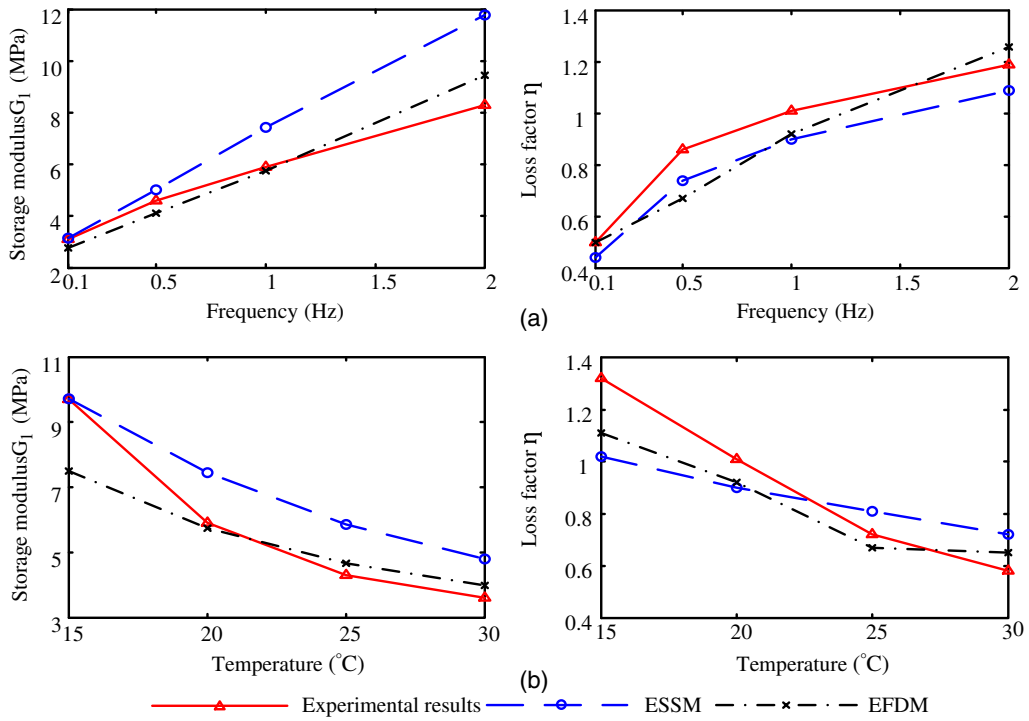

Fig. 15. Experimental and numerical results of ZN22VE material: (a) experimental and numerical results compared at temperature 20°C; (b) experimental and numerical results compared at 1-Hz frequency

the error for storage modulus is 12.8% and that for loss factor is 10%, whereas for the EFDM the error for storage modulus is 1.2% and that for loss factor is 7.5%.

It can be seen from Fig. 14(b) that the high-order EFDM is also more accurate than the ESSM when describing storage modulus G_1 and loss factor η under different temperatures. For example, when the temperature is 10°C the storage modulus experimentally is 3.0 Mpa and the loss factor is 0.71; for the ESSM the storage modulus is 3.36 MPa and the loss factor is 0.81; and for the EFDM, the storage modulus is 3.08 MPa and the loss factor is 0.67. For the ESSM the error for storage modulus is 12% and the error for loss factor is 14%, whereas for the EFDM the error for storage modulus is 2.6% and the error for loss factor is 5.6%. The detailed errors for the numerical results are listed in Table 9. It can be seen from Table 9 that the high-order EFDM is more accurate in simulating the storage modulus and loss factor of VE materials, which means that the EFDM theory can accurately describe the viscoelastic constitutive relations of VE dampers. The same conclusion can be obtained from Fig. 15 which shows comparison between experimental and numerical results for ZN22 VE material.

Conclusions

Experimental studies and numerical analysis of NBR matrix and SR matrix VE dampers were carried out. The high-order equivalent fractional derivative model, which describes the characteristics of VE dampers, is proposed and verified by the experimental data. The following conclusions can be derived from the experimental and numerical analysis:

- The hysteresis curves of the NBR matrix VE damper are relatively full, which means that the energy dissipation capacity of this damper is excellent; excitation frequency has an impact on the dynamic mechanical parameters of the NBR matrix VE damper; displacement amplitude has a slight impact on these parameters;
- The mechanical properties of the SR matrix VE damper are relatively stable under different loading conditions; excitation frequency and displacement amplitude slightly affect these properties; and
- The mechanical behavior of VE dampers can be precisely simulated by the higher-order fractional derivative model, which describes the effects of environmental temperature and excitation frequency on storage modulus and loss factor with different VE materials.

Acknowledgments

Financial support for this research is provided by National Natural Science Foundation of China (11572088), the Key Research and Development Plan of Jiangsu Province (BE2015158), Project of 973, the Science and Technological Innovation Leading Young Talents Program of the Ministry of Science and Technology, and the Fundamental Research Funds for the Central Universities of China (3205005717). This support is gratefully acknowledged.

References

Chang, K. C., Lin, Y. Y., and Lai, M. L. (1998). "Seismic analysis and design of structures with viscoelastic dampers." *ISET J. Earthquake Technol.*, 35(4), 143–166.

Chang, K. C., Soong, T. T., Oh, S. T., and Lai, M. L. (1995). "Seismic behavior of steel frame with added viscoelastic dampers." *J. Struct. Eng.*, 10.1061/(ASCE)0733-9445(1995)121:10(1418), 1418–1426.

Gluck, N., Reinhorn, A. M., Gluck, J., and Levy, R. (1996). "Design of supplemental dampers for control of structures."*J. Struct. Eng.*, 10.1061/(ASCE)0733-9445(1996)122:12(1394), 1394–1399.

Kasai, K., et al. (2008). "Value-added 5-story steel frame and its components: Part 1–Full-scale damper tests and analyses." *Proc., 14th World Conf. on Earthquake Engineering*, China Seismological Press, Beijing, China.

Kishi, H., Kuwata, M., Matsuda, S., Asami, T., and Murakami, A. (2004). "Damping properties of thermoplastic-elastomer interleaved carbon fiber-reinforced epoxy composites." *Compos. Sci. Technol.*, 64(16), 2517–2523.

Lewandowski, R., and Chorazyczewski, B. (2010). "Identification of the parameters of the Kelvin-Voigt and the Maxwell fractional models, used to modeling of viscoelastic dampers." *Comput. Struct.*, 88(1), 1–17.

Matsagar, V. A., and Jangid, R. S. (2005). "Viscoelastic damper connected to adjacent structures involving seismic isolation." *J. Civ. Eng. Manage.*, 11(4), 309–322.

Mazza, F., and Vulcano, A. (2011). "Control of the earthquake and wind dynamic response of steel-framed buildings by using additional braces or viscoelastic dampers."*Earthquake Eng. Struct. Dyn.*, 40(2), 155–174.

Min, K., Kim, J., and Lee, S. (2004). "Vibration tests of 5-storey steel frame with viscoelastic dampers." *Eng. Struct.*, 26(6), 831–839.

Park, J. H., Kim, J., and Min, K. W. (2004). "Optimal design of added viscoelastic dampers and supporting braces." *Earthquake Eng. Struct. Dyn.*, 33(4), 465–484.

Patri, M., Reddy, C. V., and Narasimhan, C. (2007). "Sequential interpenetrating polymer network based on styrene butadiene rubber and polyalkylmethacrylates." *J. Appl. Polym. Sci.*, 103(2), 1120–1126.

Payne, A. R. (2003). "The dynamic properties of carbon black-loaded natural rubber vulcanizates. Part I." *J. Appl. Polym. Sci.*, 7(3), 873–885.

Rashid, A., and Nicolescu, C. M. (2008). "Design and implementation of tuned viscoelastic dampers for vibration control in milling." *Int. J. Mach. Tools Manuf.*, 48(9), 1036–1053.

Rezaei, F., Yunus, R., and Ibrahim, N. A. (2009). "Effect of fiber length on thermomechanical properties of short carbon fiber reinforced polypropylene composites." *Mater. Des.*, 30(2), 260–263.

Saidi, I., Gad, E. F., and Wilson, J. L. (2011). "Development of passive viscoelastic damper to attenuate excessive floor vibrations." *Eng. Struct.*, 33(12), 3317–3328.

Samali, B., and Kwok, K. C. S. (1995). "Use of viscoelastic dampers in reducing wind- and earthquake-induced motion of building structures." *Eng. Struct.*, 17(9), 639–654.

Soong, T. T., and Spencer, B. F. (2002). "Supplemental energy dissipation: State-of-the-art and state-of-the-practice." *Eng. Struct.*, 24(3), 243–259.

Tsai, C. S. (1994). "Temperature effect of viscoelastic dampers during earthquakes." *J. Struct. Eng.*, 10.1061/(ASCE)0733-9445(1994)120:2(394), 394–409.

Tsai, C. S., and Lee, H. H. (1993). "Applications of viscoelastic dampers to high-rise buildings." *J. Struct. Eng.*, 10.1061/(ASCE)0733-9445(1993)119:4(1222), 1222–1233.

Xu, Z. D. (2000). "Experimental study on the (Lead) Viscoelastic structure." Ph.D. dissertation, Xi'an Architecture and Technology Univ., Xi'an, China (in Chinese).

Xu, Z. D. (2007). "Earthquake mitigation study on viscoelastic dampers for reinforced concrete structures." *J. Vib. Control*, 13(1), 29–43.

Xu, Z. D. (2011). "Model, tests and application design for viscoelastic dampers." *J. Vib. Control*, 17(9), 1359–1370.

Xu, Z. D., Zhao, H. T., and Li, A. Q. (2004). "Optimal analysis and experimental study on structures with viscoelastic dampers." *J. Sound Vib.*, 273(3), 607–618.